DEVELOPMENT AND EXPERIMENTAL ASSESSMENT OF A SOLAR COOLING SYSTEM BASED ON EJECTOR COOLING CYCLE

Konstantinos Braimakis[1]*, Spyros Kalyvas[2], Gabriel Palamidis[2], Tryfon Roumpedakis[2], Antonios Charalampidis[2], Efstratios Varvagiannis[2] and Sotirios Karellas[2]

[1]National Technical University of Athens, Laboratory of Refrigeration Air Conditioning & Solar Energy, Athens, Greece
[2]National Technical University of Athens, Laboratory of Thermal Processes, Athens, Greece

*Corresponding Author: mpraim@central.ntua.gr

ABSTRACT

The goal of the present work is the presentation of the development and experimental results of a solar cooling system based on ejector cooling cycle operating with working fluid R134a. The solar cooling system was developed in the Laboratory of Steam Boilers and Thermal Plants of NTUA and is driven by hot water at temperatures between 70 and 80°C supplied by a 48 m² solar field of selective flat plat collectors placed on the rooftop of the laboratory building capable of providing around 30 kWth and an auxiliary electric boiler. A prototype ejector device was designed and manufactured for use in the prototype based on a 1-D ejector model and following design guidelines from the literature. The performance of the system was tested at various evaporation and condensation temperatures, which were controlled through distinct hot water modules of the laboratory. According to the results of the experimental campaign, the maximum thermal coefficient of performance and ejector entrainment ratio of the system, were 0.178 and 0.21, respectively. Regardless, for achieving the maximum COP the condensation temperature of the system must be significantly low (between 24 and 26°C). For higher condensation temperatures around 30°C, the thermal COP is significantly reduced to 0.06-0.08. Furthermore, the performance of the system is highly sensitive to the evaporation temperature.

1 INTRODUCTION

Solar cooling enables the utilization of solar energy to produce cooling, thus providing the opportunity to reduce consumption of fossil fuels and greenhouse gas emissions. The first solar cooling pathway is based on photovoltaic (PV) panels coupled with a mechanically driven chiller based on a vapor compression cycle (VCC) (Karellas et al. 2018).The second pathway involves solar thermal collectors coupled with thermally-activated chillers. Such solar thermal cooling (STC) systems are based on sorption (absorption and adsorption) chillers, desiccant cooling and the ejector cooling systems. Essentially, STCs are based on substituting the mechanical compressor of the VCCs with an alternative set of thermally activated components, and as, as a result, they may have reduced electricity consumption leading to an eventual minimized environmental footprint (Roumpedakis et al. 2020). In fact, the seasonal energy efficiency ratio (EER) of STC systems, such as adsorption modules, can be as high as 15 (Palomba et al. 2019). This feature of STC systems allows for the reduction of the grid dependency and thus the consequent reduction of the power grid overloads during peak cooling demand. On the contrary, STC technologies are less mature mainly owed to the associated higher initial costs than PV-VCC systems. Regardless, they can be retrofitted to existing solar collector installations, the number of which has been rapidly increasing in the last decades, while they also have higher overall solar energy utilization efficiencies than PV-VCCs. Furthermore, they can be integrated with thermal energy storage (TES) systems, which are less expensive and environmentally friendlier storage solutions than batteries.

Among STC technologies, the main advantages of solar ejector cooling cycles (SECCs) compared to absorption chillers pertain to their simplicity, relatively low cost, higher design flexibility concerning the selection of more working fluids and low maintenance requirements, while their main drawback is

https://doi.org/10.52202/077185-0118

their lower thermal coefficient of performance (COPth) (Varga et al. 2017). All things considered, SECCs may present an appealing solution as they represent a balanced trade-off between efficiency, simplicity and cost.

In the last years, with the continuously increasing capacity of solar thermal installations, interest in SECCs is resurfacing. Many studies in the last two decades have focused on ECCs and SECCs (Tashtoush et al. 2019, Besagni 2019), with several studies focusing on experimental testing. Ruangtrakoon and Thongtip (2020) tested a standard, 3 kWc ECC operating with R141b. The evaporator and condenser temperatures were ranged from 6 to 14°C and 28 to 34°C. The performance of the test rig was evaluated for generator temperatures ranging from 80 to 105°C The optimal generator temperature was 87°C, which led to a maximum thermal COP of approximately 0.4, when the condenser and evaporator temperatures were 30°C and 10°C, respectively. Nguyen et al. (2001) tested the performance of an SECC, which was also capable of heating, operating with water as its working fluid. The nominal cooling and heating capacities of the system were 7 kWc and 20 kWth, respectively. The thermal COP of the cycle under the three tests was 0.28, 0.32 and 0.27, respectively, showing that the optimal generator temperature was 76.7°C. Śmierciew et al. (2014) carried out experiments on a standard SECC operating with isobutane. The maximum thermal COP was 0.19 and was obtained when the generator saturation temperature was 55°C for condensation temperatures below 25 °C. On the other hand, the lowest COP was observed when the primary flow saturation temperature was 63°C. Saito et al. (2014) carried out experiments on an ECC running with R134a. Four ejectors with different geometries were tested with evaporation and generation temperature of 15°C and 60°C, respectively. Jia and Wenjian (2012) tested the performance of a 2 kWc standard ECC operating with R134a for different area ratios by using an ejector with replaceable CDNs. In accordance with other studies, it was determined that as the area ratio increased, the critical backpressure decreased, with higher critical backpressures being observed at higher generator temperatures. Varga et al. (2017) conducted experimental tests of a small-scale (1.5 kWc) standard SECC with R600a. In the first set of experiments, the performance of the system considering fixed geometric parameters was monitored for a period during the day, in which the average solar irradiation was 676 W/m². During this period, the average HTF temperature was 87°C, while the generator temperature and pressure ranged from 85°C to 93°C and from 9 bar to 11.5 bar, respectively. Meanwhile, the condenser temperature ranged from 23°C to 33°C and the evaporator temperature was 6°C. The measured cooling capacity was between 1 and 2 kWc. The average thermal COP of the ECC was 0.26, reaching a maximum value of 0.40, while the electrical COP was 4.3. The authors then experimented with varying the spindle position of the VGE from 4.5 mm to 7.5 mm. The evaporator pressure was kept constant at 1.9 bar (Te=6°C) and the condenser temperature was 28°C. Overall, the maximum COP of the ECC was measured when the generator pressure was 11 bar and the SP was 5.5 mm. Besides, the authors reported that when the generator pressure was 11 bar, a COP increase by 35% was possible by adjusting the SP.

Most of the studies on ejector cooling systems focus on testing only the ejector cooling cycle and do not consider its integration with solar collectors. The goal of the present work is to present the experimental results of an integrated solar cooling system based on flat plate solar collectors coupled with an ECC that was installed in the Laboratory of Steam Boilers and Thermal Plants housed in "O" Building of the School of Mechanical Engineering at NTUA. The work was carried out in the context of the "SunClim", national funded project.

2 DESCRIPTION OF EXPERIMENTAL TEST RIG

2.1 SunClim ejector cooling cycle test rig

A brief introduction to the ECC follows before the presentation of the test-rig. The ECC (Figure 1) is like the conventional VCC, however, the mechanical compression of the latter is replaced by a dynamic compression process occurring in an ejector device. The liquid working fluid exiting the condenser is split into two flows, a primary (high-pressure) and secondary (low-pressure) flow. The primary flow is pressurized in a pump (2-3) and then heated by the heat source stream in a heat exchanger (called generator), turning into saturated or superheated hot, high-pressure vapor (3-4). Meanwhile, the secondary flow is throttled to low pressure and temperature in an expansion valve (2-5) and then

https://doi.org/10.52202/077185-0118

supplied to a heat exchanger (evaporator) in which it evaporates to produce cooling (5-6). Both the primary and secondary flows enter the ejector device through different ports. The primary flow is accelerated to supersonic speed in a converging-diverging nozzle (CDN) inside the ejector and entrains the low-pressure secondary flow exiting the evaporator. The two flows are then mixed in the process and exit the ejector device at an intermediate pressure (7). The mixed stream is driven to the condenser and is cooled down and condensed, rejecting heat in the process (7-1). Under normal operation of the ejector, both the primary and the secondary flows are choked as they enter the ejector. The subcooler does not constitute a necessary component of the cycle, however subcooling (1-2) is commonly applied in micro-scale system to prevent pump cavitation.

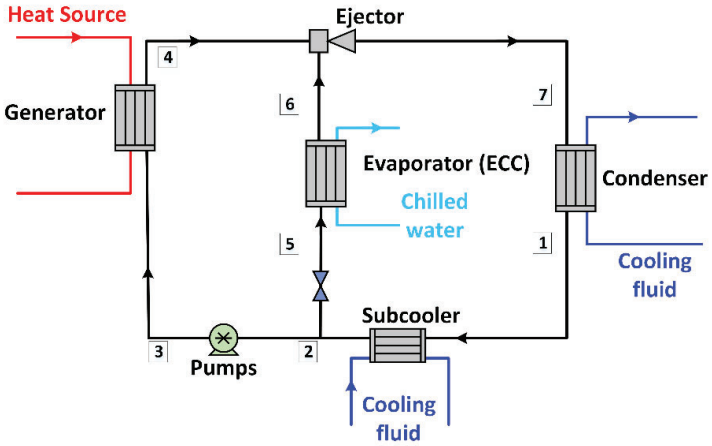

Figure 1: Ejector cooling cycle (ECC) conceptual layout

Usually, the performance of ejectors is characterized by the entrainment ratio, which is equal to the mass flow rate of the secondary flow (low-pressure entrained vapor) divided by the mass flow rate of the primary flow (high-pressure superheated vapor):

$$\omega = \frac{\dot{m}_s}{\dot{m}_p} \tag{1}$$

The ECC is a thermally driven cycle, thus the thermal and not the electrical coefficient of performance (thermal COP) is often used to assess its performance. The thermal COP is equal to the ratio of the produced cooling in the evaporator ($\dot{Q}_{evap}$) divided by the heat supplied in the generator ($\dot{Q}_{gen}$).

$$COP = \frac{\dot{Q}_{evap}}{\dot{Q}_{gen}} \tag{2}$$

The P&ID diagram of the developed ECC test rig is shown in Figure 2. The test rig is similar to the conceptual layout shown in Figure 1, however it additionally includes a bypass section which is used during start-up operation. More specifically, during start-up, the refrigerant bypasses the ejector device until its temperature at the generator outlet is sufficiently high. Furthermore, the test rig includes two parallel-connected pumps instead of a single pump to enable flexible testing under variable conditions. The experimental test rig and its control cabinet is shown in Figure 3.

https://doi.org/10.52202/077185-0118

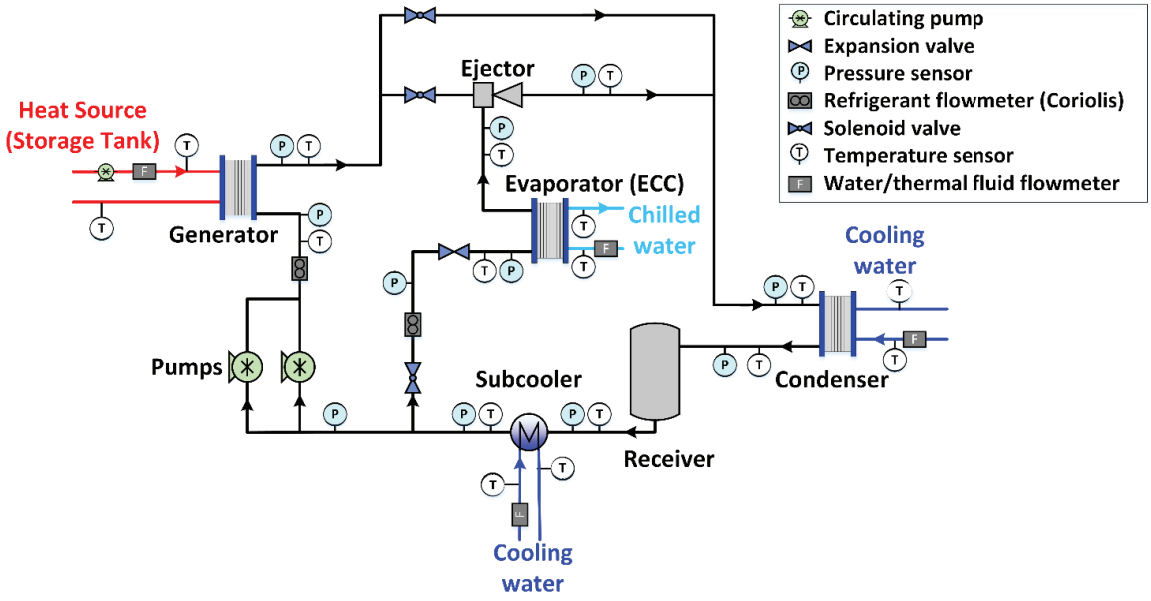

Figure 2: Ejector cooling cycle test-rig

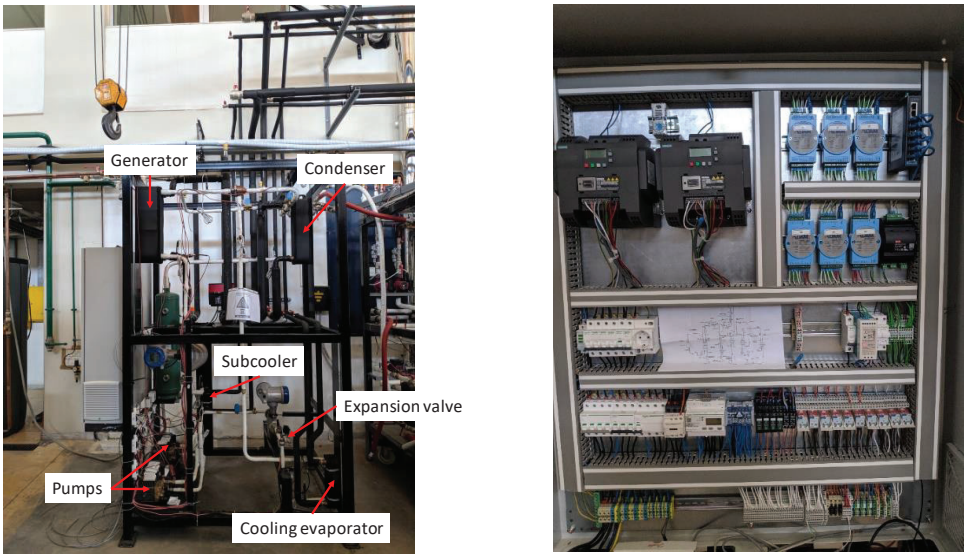

Figure 3: Ejector cooling cycle test-rig and control cabinet

An overview of the main equipment components is provided in Table 1. The SunClim ECC was designed considering a heat input from the collectors equal to approximately 30 kWth. An ECC numerical model based on the 1-D ejector model by Huang et al. (1999) was developed for determining the dimensions of the ejector (to be shown later) and calculating the specifications of the cycle (pressures, temperatures, flow rates etc.) which provided the basis for procuring the components.

https://doi.org/10.52202/077185-0118

Table 1: Main specifications of Sunclim Ejector Cooling Cycle system

Specification	**Value**
Working fluid	R134a
ECC heat input (design)	30 kW_{th}
ECC cooling evaporator heat duty (design)	4.8 kW_c
ECC condenser heat duty	34.5 kW_{th}
Primary flow pressure/temperature	19.8 bar/72°C (5 K superheating)
Secondary flow pressure/temperature	3.9 bar/10°C (2 K superheating)
Condensation pressure/temperature	8.9 bar/35°C
Evaporation temperature	8°C
Primary flow mass flow rate	0.159 kg/s
Secondary flow mass flow rate	0.030 kg/s
Ejector entrainment ratio	0.190
Thermal COP	0.161
Components	
Pumps	2 x HPE-M 04.08 piston pumps (Annovi Reverberi)
Pump motor inverters	2 x Sinamics V20 (Siemens)
Generator	ACH-70X-40M-F plate heat exchanger (Alfa Laval)
Cooling evaporator	ACH18-18H-F plate heat exchanger (Alfa Laval)
Subcooler	ACH16-14H-F plate heat exchanger (Alfa Laval)
Condenser	CB60-60H-F plate heat exchanger (Alfa Laval)
Expansion valve & controller	ETS6 electronic expansion valve (Danfoss) with EKE 1A superheat controller (Danfoss)
Measurement instruments	
Refrigerant mass flow meters	Optimass 6000 – S10 & Optimass 6000 – S08 (Khrone)

2.2 Ejector

The calculated dimensions of the ejector (Figure 4) are presented in Table 2. The ejector is composed of two components: the CDN and the constant area section (CAS)-diffuser. While the main ejector dimensions (CDN throat diameter (dt), the CDN exit diameter (d_t) and constant area section diameter (d_{CAS}) were calculated from the 1-D model, the additional dimensions were calculated based on various literature sources. The overall dimensions involve various cross-sectional areas, lengths, and angles of the two segments of the nozzle.

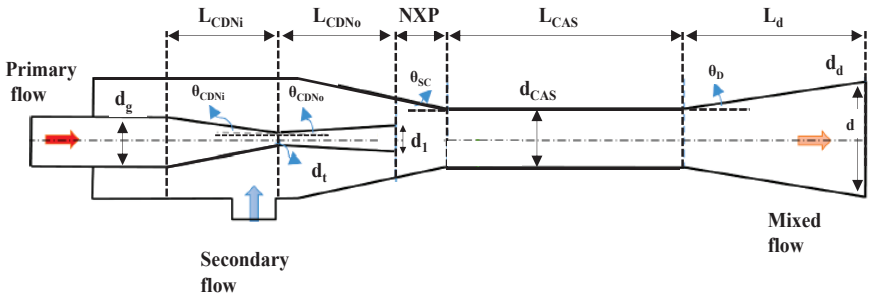

Figure 4: Ejector geometric parameters

https://doi.org/10.52202/077185-0118

Table 2: Ejector main geometrical specifications

Converging-diverging nozzle dimensions	
d_g	19.0
d_e	15.8
d_t	5.1
d_1	7
θ_{CDNi}	12
θ_{CDNo}	4
L_{CDNi}	32.8
L_{CDNo}	13.5
θ_{sc}	7.5
NXP	5.16
Constant area section dimensions	
d_{CAS}	8.6
d_d	18.2
θ_d	3.5
L_{CAS}	68.8
L_d	78.8

2.3 Solar collectors circuit

The solar collectors, Figure 5(a), were constructed by COSMOSOLAR manufacturer (Pignatelli 2011) and placed on the roof of "O" Building of the School of Mechanical Engineering of NTUA (37°58'47.4"N 23°47'06.2"E). Each solar collector has a surface of 2 m². A total of 24 flat plate collectors were used, amounting to a total solar collecting area of 48 m². The exact arrangement of the solar field is shown in Figure 5(b). As it can be observed, it consists of five distinct arrays of collectors which are connected in parallel. The two arrays close to the northern side of the rooftop consist of four collectors each, while the two arrays close to the south side of the rooftop consist of three collectors each. The fifth array, which is in the middle of the rooftop, consists of 6 collectors.

(a)

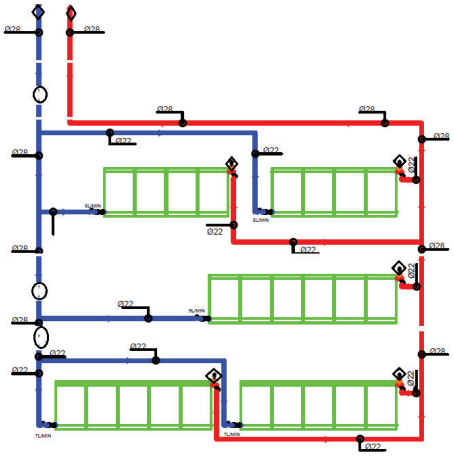

(b)

Figure 5: (a) Overview of the solar collectors field; (b) Solar field layout including five arrays of solar collectors

The heat transfer fluid (HTF) used in the solar circuit is VT-51 df by Akotec (Cocchi 2012), a water-propylene glycol mixture. As the HTF is introduced into the field (shown in blue colour), it is distributed to the 5 collector arrays, where it is heated (shown in red colour), ultimately returning to the water storage tank that is located on the ground floor of the building. Inside the tank, the hot HTF passes through a spiral heat exchanger, warming the water stored in it. Subsequently, after exiting the spiral heat exchanger, the HTF recirculates back to the solar field on the rooftop. An automated variable speed

https://doi.org/10.52202/077185-0118

circulating pump is used to regulate the flow of the HTF in the solar circuit by applying a differential control strategy. In particular, a PID controller adjusts the speed of the circulating pump to maintain a constant temperature difference between the HTF returning from the solar field and the water at the lower level inside the tank. The storage tank is connected with the generator of the ECC through a hydraulic circuit. The hot water, as shown in Figure 6. A hot water circulating pump is used for supplying water from the storage tank to the ECC generator.

Figure 6: Overview of the buffer tank and its connection to the ECC

3 EXPERIMENTAL CAMPAIGN

3.1 Goal and scope

The goal of the experimental process is to evaluate the thermal COP of the system under various operating conditions by measuring the cooling output and heat input. The controlled (independent) variables during the experimental campaign and their ranges are summarized in Table 3. The frequency of the refrigerant pumps is adjusted by their inverter. Meanwhile, the temperature and mass flow rate of the water that is supplied to the subcooler, condenser and evaporator are adjusted by the laboratory's hydraulic circuit.

Table 3: Control variables during the experimental campaign

Property	Range
Refrigerant pump frequency (Hz)	20-50
Subcooler water mass flow rate (l/min)	0-0.20
Subcooler water temperature (°C)	12.5±0.5
Condenser water mass flow rate (l/min)	0.0-1.75
Condenser water temperature range (°C)	15.0-27.0
Evaporator water mass flow rate (l/min)	0-0.20
Evaporator water temperature inlet (°C)	13.0-18.0

Heat is supplied to the system through hot water introduced into the generator from the storage tank, which is, in turn, heated by the HTF running through the solar field. The temperature of the hot water is a parameter that cannot be directly controlled during the experimental campaign, as it is determined by the thermal equilibrium of the tank. The mass flow rate of the hot water supplied to the generator was set equal to the maximum capacity of the circulating pump.

The produced cooling ($\dot{Q}_{evap}$) is calculated as the product of the measured mass flow rate of the water by its enthalpy drop (determined by its temperature measurement) at the cooling evaporator inlet/outlet. Accordingly, the heat input ($\dot{Q}_{gen}$) is then calculated as the product of the measured mass flow rate of the hot water by its enthalpy drop (determined by its temperature measurement) at the generator inlet/outlet. During all tests, the superheating degree of the working fluid at the cooling evaporator

https://doi.org/10.52202/077185-0118

outlet is controlled to a setpoint of 5 K by automatically adjusting the opening of the EEV using the valve's controller.

3.2 Results

The most important operational parameters of the ECC system are the pressure and temperature of the primary and secondary flows, as well as the pressure in the condenser, as they affect the suction ratio of the nozzle and the thermal COP of the overall system. Therefore, the presentation of experimental results is done with a particular focus on these parameters. In this context, the analysis is based on results collected during an experimental session during which the operating parameters were varied within limits indicative of the system's performance under real conditions.

More specifically, in Figure 7, the time variation of the temperature of the hot water, which is directed from the storage tank to the generator steam vaporizer for system operation (T_{hw}), is presented, along with the temperatures and pressures of the primary (P_p, T_p) and secondary flow (P_s, T_s), as well as the flow at the nozzle outlet (P_c, T_c) during the aforementioned "run". Additionally, the diagram depicting temperatures shows the time variation of the refrigerant temperature at the condenser outlet, which coincides with the condensation temperature of the refrigerant in this heat exchanger (T_{cond}), and the temperature of the refrigerant at the inlet of the cooling steam generator, generally corresponding to the vaporization temperature (saturation) of the refrigerant in this heat exchanger, given that under normal operating conditions, the refrigerant at its entry into the cooling steam generator (after leaving the expansion valve) is in a two-phase state (coexistence of liquid and gaseous phases).

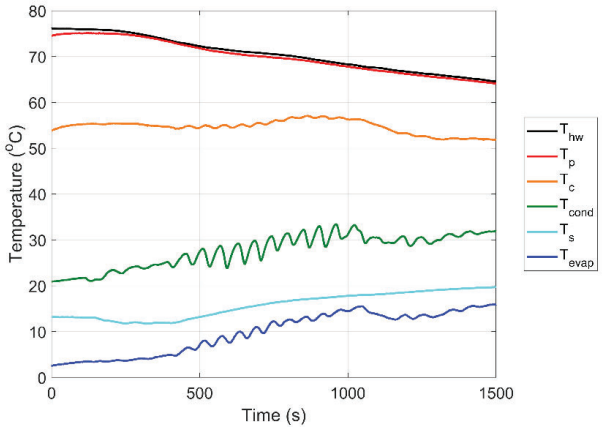

(a)

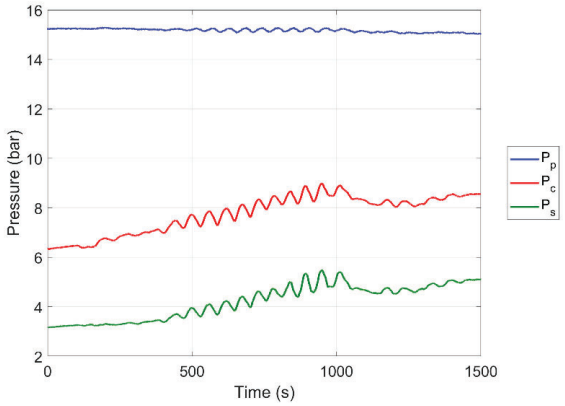

(b)

Figure 7: Time variation of temperatures and pressures of the primary flow, secondary flow, and outlet flow from the nozzle.

https://doi.org/10.52202/077185-0118

As shown in the figure, at the start of the experimental procedure, the temperature of the hot water equaled 76.1°C, as the storage tank had been fully heated by the solar fluid. During the experiment, this temperature gradually decreases, falling below 65°C, as the thermal energy of the tank is depleted since it is used to drive the ECC system. After the temperature of the tank drops below this threshold, the installation goes out of operation, as the temperature of the hot water is no longer sufficient for the ECC system to operate with satisfactory performance.

Similarly, it can be observed that the pressure of the primary flow remains almost constant at about 15.25 bar, while the temperature gradually decreases from the initial value of 75°C to 65°C. The pressure of the primary flow depends on the geometric characteristics of the nozzle and the mass flow rate of the primary flow through it. Since the mass flow rate of the primary flow remains constant due to the steady rotational speed of the pumps, the pressure also remains constant. However, the temperature of the primary flow gradually decreases due to the reduction in the temperature of the water inside the storage tank during the measurements. It is worth noting that the generator steam vaporizer operates very efficiently throughout the measurements, as the minimum temperature difference between the hot water stream and the cold refrigerant stream is very small (1-2 K). This is attributed to a slight oversizing of the corresponding heat exchanger, providing sufficient heat transfer surface to rapidly adapt to temperature gradients.

Given that the pressure of the primary flow is constant while the temperature varies, it follows that the degree of superheating of the primary flow is not constant but varies during the measurements. The degree of superheating results from the difference between the temperature of the primary flow and the vaporization temperature (saturation) within the generator steam vaporizer, which is (for the almost constant vaporization pressure of 15.2 bar) equal to 55°C. Therefore, the degree of superheating roughly ranges between 0.17 and 15 K.

The pressure and temperature of the secondary flow are determined by the opening of the expansion valve with the requirement of constant superheating, as well as by the temperature of the supplied cooling water to the cooling steam generator. During measurements, the temperature varies from a minimum value of 13°C to a maximum value of 20°C. Additionally, the pressure increases from 3 bar to a maximum value of 5 bar. The variation in the pressure and temperature of the secondary flow is due to a gradual increase in the temperature of the cooling water in the cooling steam generator, aiming to investigate the system's behavior under changing operating conditions. Based on the vaporization temperature of the refrigerant in the cooling steam generator, the degree of superheating of the refrigerant in this heat exchanger ranges between 1 and 8 K, depending on the operating conditions. It is reminded that the degree of superheating is determined by the controller of the expansion valve, which controls its opening to achieve a degree of superheating of 5 K.

Figure 8 presents the corresponding performance results for the estimated COP (blue line) and the entrainment ratio (red line). The maximum reported COP was equal to 0.178. As seen in Figure 8, after the first 600 s of the experimental procedure, a decline in the COP was observed, which was mainly associated to the respective depletion of the driving heat from the storage tank and the simultaneous increase in the inlet temperature of the cooling water. With respect to the entrainment ratio, the maximum reported value was 0.212. The highest values of the entrainment ratio were also reported during the first part of the experimental procedure, owing to the lower values of the condensation temperature. As the condensation temperature steadily increased, the entrainment ratio declined. At this point is important to clarify, that the regions of zero entrainment ratio, in Figure 8, are associated with transient periods of a closed expansion valve.

https://doi.org/10.52202/077185-0118

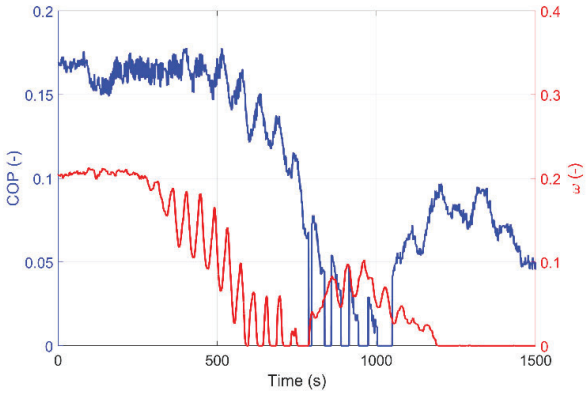

Figure 8: Time variation of temperatures and pressures of the primary flow, secondary flow, and outlet flow from the nozzle.

4 CONCLUSIONS

In this study, the development, sizing and preliminary experimental characterization of a solar driven ECC system is discussed. The main conclusions of the study are the following:

- A total of 48 m2 flat plate collectors was installed in Athens, Greece, to drive the ECC system, with a nominal heat input of 30 kW. A 1 m³ storage tank was installed to store the solar heat and serve as an intermediate loop to absorb any irradiance discrepancies, ensuring a steady profile driving heat for the ECC.
- A dedicated ejector was designed and installed in the ECC test rig for experimental characterization.
- An experimental procedure was implemented to evaluate the performance of the ECC system with respect to the estimated COP and the achieved entrainment ratio of the ejector.
- The reported thermal COP of the ECC reached a value of 0.178, which is considered a reasonable value for a generation temperature of almost 76 ºC. As the available heat decreased, causing a decline in the generation temperature, the measured COP began to decrease as well.
- The entrainment ratio reaches values as high as 0.21, for lower condensation and higher generation temperatures. An increase in the condensation temperature has a negative effect on the entrainment ratio of the ECC.

NOMENCLATURE

COP	Coefficient of performance	(-)
d	Diameter	(m)
h	specific enthalpy	(J/kg)
L	length	(m)
$\dot{m}$	mass flow rate	(kg/s)
P	Pressure	(bar)
$\dot{Q}$	heat duty	(W)
T	Temperature	(K)

Subscript

Δ	difference	(-)
η	efficiency	(-)
θ	angle	(deg)
ρ	density	(kg/m³)
ω	entrainment ratio	(-)

https://doi.org/10.52202/077185-0118

Subscript

c	ejector's nozzle outlet
cond	condenser
evap	evaporator
gen	generator (heat exchanger)
hw	hot water
p	primary flow
s	secondary flow
th	thermal

Abbreviations

CAS	constant area section
CDN	converging-diverging nozzle
ECC	Ejector Cooling Cycle
EEV	electronic Expansion Valve
HTF	Heat transfer fluid
NXP	nozzle exit position
PV	photovoltaic
SECC	solar ejector cooling cycles
STC	solar thermal cooling
TES	thermal energy storage
VCC	Vapor Compression Cycle

REFERENCES

Besagni, G. 2019. "Ejectors on the cutting edge: The past, the present and the perspective." *Energy* 170:998-1003.

Cocchi, M. 2012. IEA Bioenergy Task 40: Country profile Italy 2011. edited by ETA Florence.

Huang, B.J., Chang, J.M., Wang, C.P., and Petrenko, V.A. 1999. "A 1-D analysis of ejector performance." *International Journal of Refrigeration* 22 (5):354-364.

Jia, Y., and Wenjian, C. 2012. "Area ratio effects to the performance of air-cooled ejector refrigeration cycle with R134a refrigerant." *Energy Conversion and Management* 53 (1):240-246.

Karellas, S., Roumpedakis, T.C., Tzouganatos, N., and Braimakis, K. 2018. *Solar Cooling Technologies*: CRC Press.

Nguyen, V.M., Riffat, S.B., and Doherty, P.S. 2001. "Development of a solar-powered passive ejector cooling system." *Applied Thermal Engineering* 21 (2):157-168.

Palomba, V., Wittstadt, U., Bonanno, A., Tanne, M., Harborth, N., and Vasta, S. 2019. "Components and design guidelines for solar cooling systems: The experience of ZEOSOL." *Renewable Energy* 141:678-692.

Pignatelli, V., Alfaro,V. 2011. Bioenergy industry and markets in Italy. edited by Energy and sustainable economic development Italian National Agency for New technologies.

Roumpedakis, T.C., Kallis, G., Magiri-Skouloudi, D., Grimekis, D., and Karellas, S. 2020. "Life cycle analysis of ZEOSOL solar cooling and heating system." *Renewable Energy* 154:82-98.

Ruangtrakoon, N., and Thongtip, T. 2020. "An experimental investigation to determine the optimal heat source temperature for R141b ejector operation in refrigeration cycle." *Applied Thermal Engineering* 170:114841.

Saito, Y., Ito, T., Matsuo, A., and Sato, H. 2014. "Ejector Configuration for Designing a Simple and High Performance Solar Cooling System." *Energy Procedia* 57:2564-2571.

Śmierciew, K., Gagan, J., Butrymowicz, D., and Karwacki, J. 2014. "Experimental investigations of solar driven ejector air-conditioning system." *Energy and Buildings* 80:260-267.

Tashtoush, B.M., Al-Nimr, M.d.A., and Khasawneh, M.A. 2019. "A comprehensive review of ejector design, performance, and applications." *Applied Energy* 240:138-172.

https://doi.org/10.52202/077185-0118

Varga, S., Oliveira, A.C., Palmero-Marrero, A., and Vrba, J. 2017. "Preliminary experimental results with a solar driven ejector air conditioner in Portugal." *Renewable Energy* 109:83-92.

ACKNOWLEDGEMENT

The work has received funding from the General Secretariat of Research and Innovation (GSRI) of in the context of the SunClim project (T1EΔK-04359) of the "Research-Create-Innovate" action of the "Competitiveness, Enterpreneurship & Innovation (EPAnEK) programme.

https://doi.org/10.52202/077185-0118